

# Event-Guided Rolling Shutter Correction with Time-Aware Cross-Attentions

Anonymous Authors

## ABSTRACT

Many consumer cameras with rolling shutter (RS) CMOS would suffer undesired distortion and artifacts, particularly when objects experiences fast motion. The neuromorphic event camera, with high temporal resolution events, could bring much benefit to the RS correction process. In this work, we explore the characteristics of RS images and event data for the design of the rolling shutter correction (RSC) model. Specifically, the relationship between RS images and event data is modeled by incorporating time encoding to the computation of cross-attention in transformer encoder to achieve time-aware multi-modal information fusion. Features from RS images enhanced by event data are adopted as keys and values in transformer decoder, providing source for appearance, while features from event data enhanced by RS images are adopted as queries, providing spatial transition information. By embedding the time information of the desired GS image into the query, the transformer with deformable attention is capable of producing the target GS image. To enhance the model's generalization ability, we propose to further self-supervise the model by cycling between time coordinate systems corresponding to RS images and GS images. Extensive evaluations over both synthetic and real datasets demonstrate that the proposed method performs favorably against state-of-the-art approaches.

## CCS CONCEPTS

• Computing methodologies → Computer vision; Reconstruction.

## KEYWORDS

Event Camera, Multi-Modality, Image Enhancement, Rolling Shutter Correction, Self-supervised Training

## 1 INTRODUCTION

Many consumer cameras, such as smartphone cameras, employ a rolling shutter (RS) CMOS sensor for power and cost consideration. The rolling shutter camera sensor exposes asynchronously in a row-by-row manner while the global shutter exposes at all positions simultaneously. Hence the images based on RS exposure would suffer image distortion and occlusion problems, which is called jelly effect, particularly when objects experience fast motion. To remove such artifacts in an image caused by rolling shutter and recover a

distortion-free GS image, various rolling shutter correction (RSC) techniques are developed.

The task of rolling shutter correction is challenging because it is difficult to estimate the transformation between RS and GS images especially when rolling shutter is coupled with both object motion and camera motion. It is a highly ill-posed problem for RSC from a single image due to the absence of motion information. Hence, there have been several works [5, 15, 31] proposed to first estimate motion fields between consecutive frames and compute correction fields based on them, which is followed by applying warping operation to the RS images for GS image recovery.

However, most of them exhibit poor performance when confronted with complex motion because of simple motion assumption during exposure.

Event camera, a bio-inspired sensor that outputs event signal with high temporal resolution (in the order of  $\mu\text{s}$ ) by asynchronously measuring brightness change at each pixel [6], could provide much complementary information for the RSC task. By synergizing a RGB camera and an event camera, the triggered events are able to record how intensity at each pixel evolves during exposure of RGB camera. They carry abundant information about motion happened in the scene. Hence, making full use of events could bring much benefit to the process of rolling shutter correction. There have been a few attempts along this direction. Zhou *et al.* [32] present a two-branch approach to leverage events for RSC. For the synthesis branch row-wise readout time offsets are injected into attention and fused with RS frame to restore a GS image, while for the warping branch events join the estimation of flow between RS and GS images and obtain another GS image. The two estimated GS images are further combined to give the final GS restoration result. In [1] a transformation is conducted to encode only events between readout time of RS and GS such that row-wise motion can be directly estimated without constant linear motion assumption. It also takes two-branch framework and uses the fusion result as the final prediction. However, the way that they use the events and row-wise readout time for correcting rolling shutter effect, *i.e.*, either directly injecting time offsets to event representation or selecting only events between RS and GS as input, might not be optimal. Involving row-wise readout time in the interaction between RS images and events could help explore more potential of events for the RSC task.

In this work, we present an event-assisted encoder-decoder framework for rolling shutter correction. In the encoding stage, the RS frame and event data are first respectively sent to a separate convolutional layer for shallow feature extraction. They are then separately fed to several transformer layers which are equipped with the proposed time-aware multi-head attention for cross-modal feature enhancement. Since time encodings play different roles in the feature enhancement for each modality, different forms of time encodings are exploited. For the RS image, row-wise time encodings are used because each row in the RS image correspond to the same exposure time; while for event data, channel-wise time encodings

Permission to make digital or hard copies of all or part of this work for personal or

Unpublished working draft. Not for distribution. distributed for profit or commercial advantage and that copies bear this notice and the full citation on the first page. Copyrights for components of this work owned by others than the author(s) must be honored. Abstracting with credit is permitted. To copy otherwise, or republish, to post on servers or to redistribute to lists, requires prior specific permission and/or a fee. Request permissions from [permissions@acm.org](mailto:permissions@acm.org).

ACM MM, 2024, Melbourne, Australia

© 2024 Copyright held by the owner/author(s). Publication rights licensed to ACM.

ACM ISBN 978-x-xxxx-xxxx-x/YY/MM

<https://doi.org/10.1145/nnnnnnn.nnnnnn>

59  
60  
61  
62  
63  
64  
65  
66  
67  
68  
69  
70  
71  
72  
73  
74  
75  
76  
77  
78  
79  
80  
81  
82  
83  
84  
85  
86  
87  
88  
89  
90  
91  
92  
93  
94  
95  
96  
97  
98  
99  
100  
101  
102  
103  
104  
105  
106  
107  
108  
109  
110  
111  
112  
113  
114  
115  
116

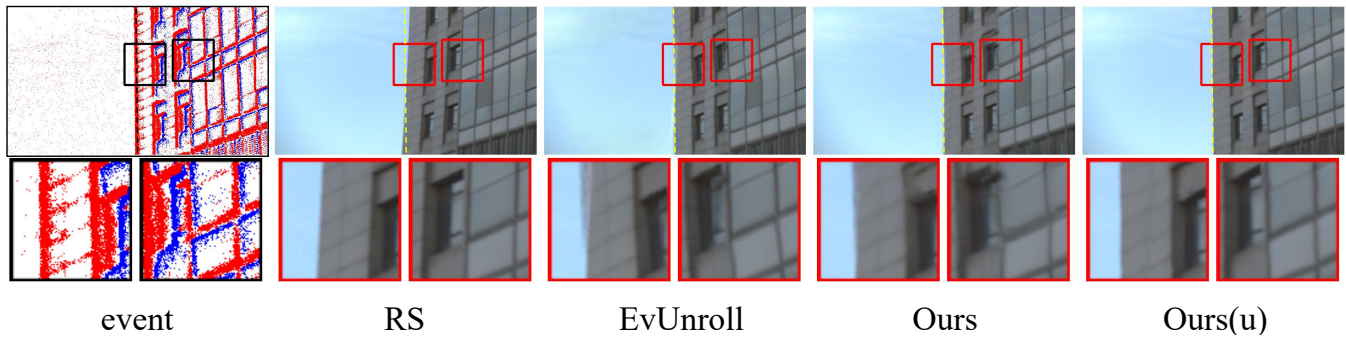


**Figure 1: An example of rolling shutter correction on real-world data compared with sota method EvUnroll [32]. The yellow dashed line is the GS reference line drawn based on the intermediate event. The label (u) means fine-tuning using self-supervised learning.**

are used due to the use of voxel grid representation. We utilize this characteristic to design time encoding and combine it with multi-head attention to better integrate the information from both modality. In the decoding stage, we produce the corresponding GS image at the desired time stamp. Due to the significant image displacement in the RSC task, directly reconstructing the image from features can be challenging. To address this, we utilize Deformable Cross Attention (DCA) [34] to expand receptive field. By taking both event features and GS time encoding as the queries and RS features as keys, DCA can effectively leverage the motion information with events and appearance information with RS frame to reconstruct a GS image.

Moreover, to improve the model’s generalization ability, we designed a self-supervised method with single RS image and event specifically for the RSC task. This method enables us to fine-tune the model on test datasets and real datasets. In summary, our contributions are as follows:

- We proposed a novel architecture specifically designed for the characteristics of the RSC task.
- We proposed a self-supervised loss tailored for the RSC task to enhance the model’s generalization and improve its performance on real-world datasets.
- Our method outperforms existing methods in both qualitative and quantitative performance.

## 2 RELATED WORKS

### 2.1 Rgb-based RSC methods

Multiple images methods mostly predict optical flow between two consecutive images according linear motion assumption. Fan *et al.* [2, 4] proposed to calculate optical flow in stage one, and then obtain the final GS image with warped image in stage two, which is similar to the [9] structure. DSUN [15] and SUNet [3] calculate cost volume for multi-scale pyramid features respectively, and distort and fuse the features to restore GS image. JCD [31] simultaneously processes RSC and deblurring tasks by using deformable attention module to fuse bidirectional warped features. Naor *et al.* [17] regarded the RS correction problem as a temporal upsampling problem and proposed additional supervision at the x-t level. Fan *et al.* [5] proposed a single-stage architecture which combines

appearance refinement and undistortion motion estimation for efficient RS correction. Zhong *et al.* [30] adopted a novel setup where two RS images are scanned in different directions (from top to bottom and from bottom to top) simultaneously, extracting symmetrical information for GS recovery. Building upon the same setup, a bidirectional warping module was designed to restore original RS images in [19], followed by self-supervised training based on temporal consistency.

### 2.2 Multi-modality image enhancement

The rich temporal information of events enables them to perform many image enhancement tasks, such as deblurring [10, 14, 18, 20–22, 27, 29], frame interpolation [7, 12, 23, 24, 26], and RSC [1, 32]. REDNet [27] achieves self-supervised deblurring by unfolding a blurry image into multiple sharp images and introducing optical flow constraints between each sharp image. TimeReplayer [7] uses a structure similar to SuperSloMo to interpolate an image from two input images, and one input image and the resulting image can be extrapolated to another input image, achieving self-supervised results. EVDI [29] uses two blurry images taken at different times to restore a sharp image at the same timestamp, achieving self-supervised results. These self-supervised methods mostly rely on either a single blurry image or multiple sharp images.

TimeLens [24] is the first to use both the motion information and the physical properties of event, and it employs two branches for warping and synthesis to perform frame interpolation. EvUnroll [32] uses a similar two-branch structure to handle the RSC problem, reflecting the different time relationships of each row in RS by changing the timemap during warping branch. EvShutter [1] captures the events between RS and GS and estimates the optical flow between RS and GS without using the linear motion assumption.

## 3 METHOD

Here we first briefly introduce preliminary knowledge about event representation and formation of rolling shutter images. Then we will explain how spatio-temporal relationship among events, RS images and GS images could be leveraged in the encoder-decoder framework for event-assisted rolling shutter correction. Finally, the supervision imposed on the model training is presented, which also

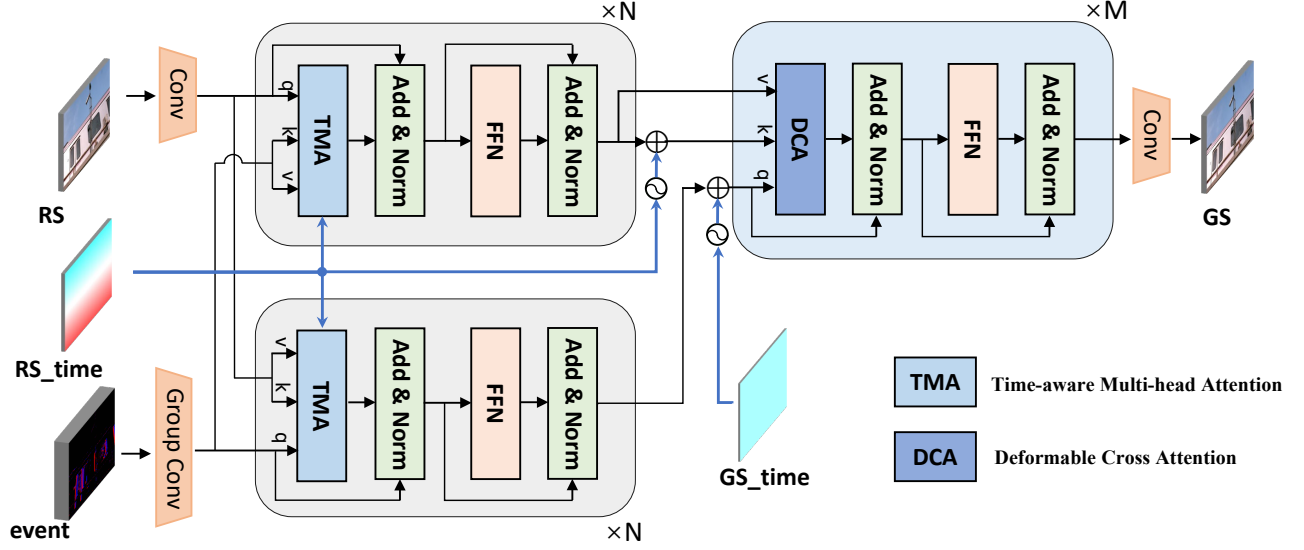


Figure 2: Overview of our network architecture.

include both supervised losses and the proposed self-supervised loss.

### 3.1 Preliminary

In an event camera, when the intensity variance of a certain pixel between consecutive time stamps reaches a threshold  $C$ , an event with a certain polarity would be triggered. Typically, a stream of events over a period of time can be represented as:

$$\mathcal{E} = \{e_i\}_{i=1}^N = \{(x_i, y_i, t_i, p_i)\}_{i=1}^N, \quad (1)$$

where  $t$  is the triggered time stamp,  $(x, y)$  represents the triggered pixel position, and  $p$  represents its polarity. A popular way to represent event set is to transform those events into voxel grids [33] as shown below:

$$E(x_l, y_m, t_i) = \sum_{\substack{x_i=x_l \\ y_i=y_m}} p_i \max(0, 1 - |t_i - t_i^*|), \quad (2)$$

where  $t_i^* \triangleq \frac{B-1}{\Delta T} (t_i - t_0)$  represents the normalized time slices. In voxel grids, events are accumulated in adjacent time slices such that each time slice could contain information at different times. Compared with other event representation such as record the quantity and the last moment of the event, voxel grid contains more detailed temporal information.

A rolling shutter image can be treated as a stack of rows of a global shutter image with each one exposed at different time stamps. Even a small object motion or camera motion would cause distortion in the rolling shutter image. Hence a rolling shutter image can be formulated as below:

$$I_{RS}^{(t)} = \sum_{h=1}^H I_{GS}^{(t+(h-M/2)t_r)} [h], \quad (3)$$

where  $t_r$  denotes the readout time between consecutive rows;  $M$  denotes the number of rows;  $t + (h - M/2)t_r$  means the exposure

time of the  $h$ -th row. Since GS are sharp images captured with short exposure time, here the temporal information is represented by the mid-exposure moment rather than the start and end of exposure.

### 3.2 Method

As shown in Fig. 2, the overall model is an encoder-decoder based framework composed of transformers. In encoder, we employ transformers with the proposed Time-Aware Multi-head Attention to model the spatio-temporal relationship among RS images, events and GS images to obtain multimodal features for later GS image decoding. In decoder, we used DCA to extract the appearance information of RS features based on the timestamp of GS, utilizing the motion information of the event features. The network takes a stream of events and an RS image with its exposure parameters as inputs, outputting GS images at any time within the time interval.

#### Encoder with Time-aware Multi-head Attention

Events record almost all continuous brightness change during the exposure time, from the beginning time stamp of the first row of a RS image to the end time stamp of its last row. Such brightness change could be caused by either motion or dynamic lighting. In this task we expect to explore the value of motion information associated with events in the entire exposure period. The encoder starts with a few convolutional layers for shallow feature extraction of the RS frame, while for event data group convolution operation is conducted to retain time ordering information. Simply concatenating representations of two modalities might not be suitable because the features of two modalities are neither spatially aligned nor temporally synchronized. This would cause significant burden to the network in later information fusion and feature enhancement. To fully make use of motion information with event data for RSC, we first resort to powerful transformers to enhance features of both RS frame and events with help of each other. We design a novel Time-aware Multi-head Attention (TMA) for the transformer layer

to enhance each modality. The design principle is to take timing information as a bridge between the modalities of RS frame and event stream.

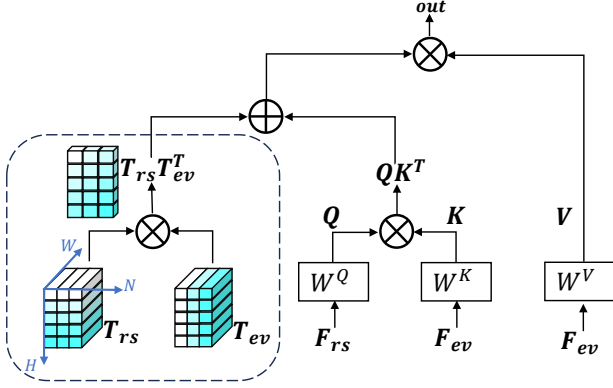


**Figure 3: Time-awareness Multi-head Attention.**

Inspired by the positional encodings in most transformers [25], here we propose to use time encodings in the transformer and leverage them to promote mutual enhancement. As for features of the RS frame  $\mathcal{F}_{rs} \in \mathbb{R}^{B \times C \times H \times W}$ , its rows correspond to a set of consecutive readout time stamps. Therefore we can directly assign a row-dependent time encodings to RS features. Since each column has the same readout time, we simply denote the time encoding for RS frame as  $\mathcal{T}_{rs}^{h,w} = \text{sinusoid}(\frac{h}{H})$ ,  $h \in [0, H]$ ,  $w \in [0, W]$ , where *sinusoid* represents the sinusoidal positional encoding, represented as:

$$\begin{aligned} \text{sinusoid}(p)[2i] &= \sin(p/10000^{2i/C}), \\ \text{sinusoid}(p)[2i+1] &= \cos(p/10000^{2i/C}), \end{aligned} \quad (4)$$

where  $i = (0, \dots, C/2 - 1)$ .

While as for the voxel-grid-like representation of event data  $\mathcal{F}_{ev} \in \mathbb{R}^{B \times C \times H \times W}$ , groups along channel correspond to consecutive temporal intervals. Therefore, we divide the event features into  $N$  groups along channel, with each one corresponding to certain temporal range. Group-channel-wise time encodings are assigned to event features, which can be denoted as  $\mathcal{T}_{ev}^{h,w,i} = \text{sinusoid}(\frac{i}{N})$  and  $\mathcal{T}_{ev}^{h,w} = \text{concat}([\mathcal{T}_{ev}^{h,w,i}])$ ,  $i = (0, \dots, N-1)$ . To promote interaction between RS features and event features, time encodings of each modality are combined with the corresponding modality features in computation of cross-attention. Inspired by [16], query or key features are concatenated with time encodings and the cross-attention could be computed as below:

$$\text{attention} = \text{SoftMax}((QK^T + \mathcal{T}_{rs}\mathcal{T}_{ev}^T)/\sqrt{d})V \quad (5)$$

However, it is not proper to directly compute the product of  $\mathcal{F}_{rs}$  and  $\mathcal{F}_{ev}$  because each time encoding vector for RS frame corresponds to one timestamp while each time encoding vector for event data corresponds to multiple timestamps. Hence we take inspiration from multi-head cross-attention and present time-aware multi-head attention to address this issue. Here we will take the case of RS features as queries and event features as keys and values as an example to explain how Time-aware Multi-head Attention (TMA) works. Since each group of  $C/N$  channels in the

time encodings for event features corresponds to a certain temporal range, the dimension of time encodings for RS features are also set to  $C/N$ . In this way time encodings of two modalities could be easily compared and their similarity could also be measured through product. The  $i$ -th group event time encodings is  $\mathcal{T}_{rs}^{h,w,i} = \text{sinusoid}(\frac{i}{N}) \in \mathbb{R}^{B \times C/N \times H \times W}$ , and the  $i$ -th group RS time encodings is  $\mathcal{T}_{ev}^{h,w,i} = \text{sinusoid}(\frac{h}{H}) \in \mathbb{R}^{B \times C/N \times H \times W}$ . In this way, both RS and event features are divided into sub-features similar to the heads in standard multi-head attention, we can compute the product of RS and event time encodings in a time-wise way within each head. Correspondingly, RS features and event features are also divided into  $N$  sub-features which are denoted as  $\mathcal{F}_{rs}^i$  and  $\mathcal{F}_{ev}^i$ . Then as shown in Fig 3, time-aware multi-head attention can be represented as:

$$\text{MHA}(Q, K, V) = \text{Concat}(\text{head}^1, \dots, \text{head}^N)W^O, \quad (6)$$

where  $\text{head}^i = \text{SoftMax}((Q^i K^{iT} + \mathcal{T}_{rs}^i \mathcal{T}_{ev}^{iT})/\sqrt{d})V^i$ , and  $Q^i = \mathcal{F}_{rs} W_i^Q$ ,  $K^i = \mathcal{F}_{ev} W_i^K$ ,  $V^i = \mathcal{F}_{ev} W_i^V$ ,  $d = C/N$ . As for the case of event features as queries and RS as keys and values, the computation is similar. In summary, by dividing temporal encodings and features for RS frame and event data into multi-heads, TMA is able to effectively integrate temporal relationship between the two modalities into the cross-attention for cross-modal enhancement.

### Decoder with Deformable Cross Attention

In the encoding stage, information associated with RS frame and event data is sufficiently explored and fused. The decoder aims at predicting the desired GS image in the middle exposure period or at any specified time stamp based on the enhanced features from encoder. Since there is often significant misalignment between RS and GS frames, we employ deformable cross-attention in the decoder to expand receptive fields and accelerate model convergence. The queries of the deformable cross-attention consist of two components, *i.e.*, enhanced event features from the encoder and the time encoding for desired GS time stamp. The enhanced RS features from the encoder are used as the keys and values of the attention. In this way the desired time and rich motion information provided by event features work as guidance and complement to remove spatial distortion in RS features. Then a GS image is recovered from the spatially corrected RS features with another few convolutional layers.

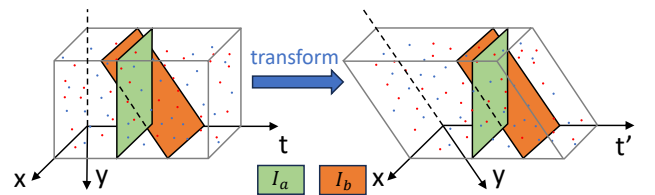


**Figure 4: temporal reference system transform.**

### 3.3 Supervision for Rolling Shutter Correction

The supervision for our RSC framework include both supervised reconstruction loss and a proposed self-supervised loss. We first introduce the proposed self-supervised loss. As shown in Fig. 1,

given a pair of RS and GS images  $I_a$  and  $I_b$ , can we determine which one is RS image and which one is GS image? Obviously, we cannot. Without a prior assumption like "lines must remain straight", we cannot determine if an object appears curved due to rolling shutter effect or if it was originally shaped in that way.

Actually, we could have two different time reference systems based on either GS  $t_{gs}^i$  or RS  $t_{rs}^i$ . In the GS time reference system, each row in GS image  $I_a$  has the same exposure time while each row in RS image  $I_b$  has different time as shown below:

$$\begin{aligned} I_a : t_{gs}^{a,1} &= t_{gs}^{a,2} = \dots = t_{gs}^{a,H}, \\ I_b : t_{gs}^{b,i} &= t_{gs}^{b,1} + (i-1) * \delta, \end{aligned} \quad (7)$$

where  $t_{gs}^{a(b),i}$  represents the  $i$ -th row's exposure time with respect to GS time reference system,  $i \in [1, \dots, H]$ ,  $\delta$  denotes the readout time delay between successive rows in  $I_b$ .

In the RS time reference system, each row in  $I_b$  has the same exposure time while the one in  $I_a$  has different time as shown below:

$$\begin{aligned} I_a : t_{rs}^{a,i} &= t_{rs}^{a,1} - (i-1) * \delta, \\ I_b : t_{rs}^{b,1} &= t_{rs}^{b,2} = \dots = t_{rs}^{b,H}, \end{aligned} \quad (8)$$

where  $t_{rs}^{a(b),i}$  represents the  $i$ -th row's exposure time with respect to RS time reference system. The relation between the two time reference systems can be represented in the transform as shown in Eq. 9 and Fig 4.

$$t_{rs}^i = f(t_{gs}^i) = t_{gs}^i + (i-1) * \delta + b, \quad (9)$$

where  $b$  represents the inception. The choice of time reference system would affect the use of event data because every event is represented with a quadruplet  $(t, x, y, p)$  including its time stamp, position, and polarity. By transforming the time value in the event quadruplets, we convert events from one temporal coordinate system to another, which are respectively denoted as  $e$  and  $e'$  as shown below.

$$e(t_{gs}, x, y, p) = e'(t_{rs}, x, y, p). \quad (10)$$

Assume we have a pre-trained rolling shutter correction model  $f_{RSC}$ . By introducing the idea of cycling transform, we could construct a self-supervision loss. Firstly, in the GS time reference system, the RS image  $I_a$  with RS and GS timestamp is sent to the RSC model to predict a GS image  $I_{o1}$ .

$$I_{o1} = f_{RSC}(I_a, e, t_{gs}^a, t_{gs}^b) \quad (11)$$

By switching to RS time reference system and considering  $I_{o1}$  as the input "RS image", we can apply the RSC model again to recover a "GS image" with help of events  $\{e\}$ .

$$I_{o2} = f_{RSC}(I_{o1}, e', t_{rs}^a, t_{rs}^b) \quad (12)$$

The recovered "GS image"  $I_{o2}$  in RS time reference system should be identical to the original RS image  $I_{rs}$  in GS time reference system. Hence the self-supervised loss function could be computed as follows:

$$\mathcal{L}_{self} = \|I_{rs} - I_{o2}\|_1. \quad (13)$$

We provide an x-t plot in the supplementary materials for a better understanding of self-supervised learning.

Finally, our loss function consists of a Charbonnier loss [?] to reconstruct GT, a perceptual loss [11], and a self-supervised loss.

$$\mathcal{L} = \mathcal{L}_{error} + \alpha \mathcal{L}_{photo} + \beta \mathcal{L}_{self} \quad (14)$$

## 4 EXPERIMENTS

In Section 4.1, we validate the effectiveness of the design module through ablation experiments. Subsequently, in Sections 4.2 and 4.3, we will compare with existing methods on RSC benchmark datasets. Finally, we will examine the effectiveness of self-supervised effectiveness on different methods and both synthetic and real datasets.

Table 1: Ablation study

Methods	PSNR	SSIM
SwinIR [13]	30.83	0.88
w/o TMA	32.87	0.91
w/o DCA	32.18	0.91
ours	<b>33.53</b>	<b>0.92</b>

### 4.1 Ablation study

To examine the effectiveness of TMA, we experiment with another simpler time encoding without the design of multi-head attention focusing on events at different time periods. In this approach, RS time encoding is generated based on the exposure time of each row with the same size as the RS feature ( $t_{rs}, \mathcal{F}_{rs} \in \mathbb{R}^{B \times C \times H \times W}$ ), and event time encoding is generated by the mid-exposure time of RS with the same size as the event feature as well ( $t_{ev}, \mathcal{F}_{ev} \in \mathbb{R}^{B \times C \times H \times W}$ ). And their product is add to the product of query and key as Eq. 5.

To validate the importance of receptive field in the RSC task, we conduct a comparative experiment where we replace deformable attention with normal attention. Additionally, we provide a reference experiment with SwinIR to verify if the encoder-decoder structure is better. For SwinIR, we directly concatenate RS, event, and timemap together as the input of the original SwinIR architecture.

As shown in Tab. 1, compared with original SwinIR architecture, our time encoding based encoder-decoder structure performance is better. This is because without query based decoder, it's hard to build difficult to establish the temporal relationship between RS, GS, and events. Just concatenating all these as inputs can't fully integrate the temporal information of the two modalities. Without deformable attention, there is noticeable decrease in PSNR. This is mainly due to two reasons. First, the network lacks a sufficient receptive field, resulting in failure to recover in scenes with large RS offsets, such as high-speed motion, leading to residual RS artifacts. Additionally, the use of regular cross-attention does not effectively exploit the characteristics of each modality, and the motion information of events is not fully utilized. In addition to its effectiveness, using DCA can also lead to reduced computational complexity and accelerated training. Using a different time encoding instead of TMA will also result in a certain decrease in PSNR. That is because this type of encoding of RS represents only a small time interval at each position while event time encoding represents the entire exposure duration. When performing cross-modality

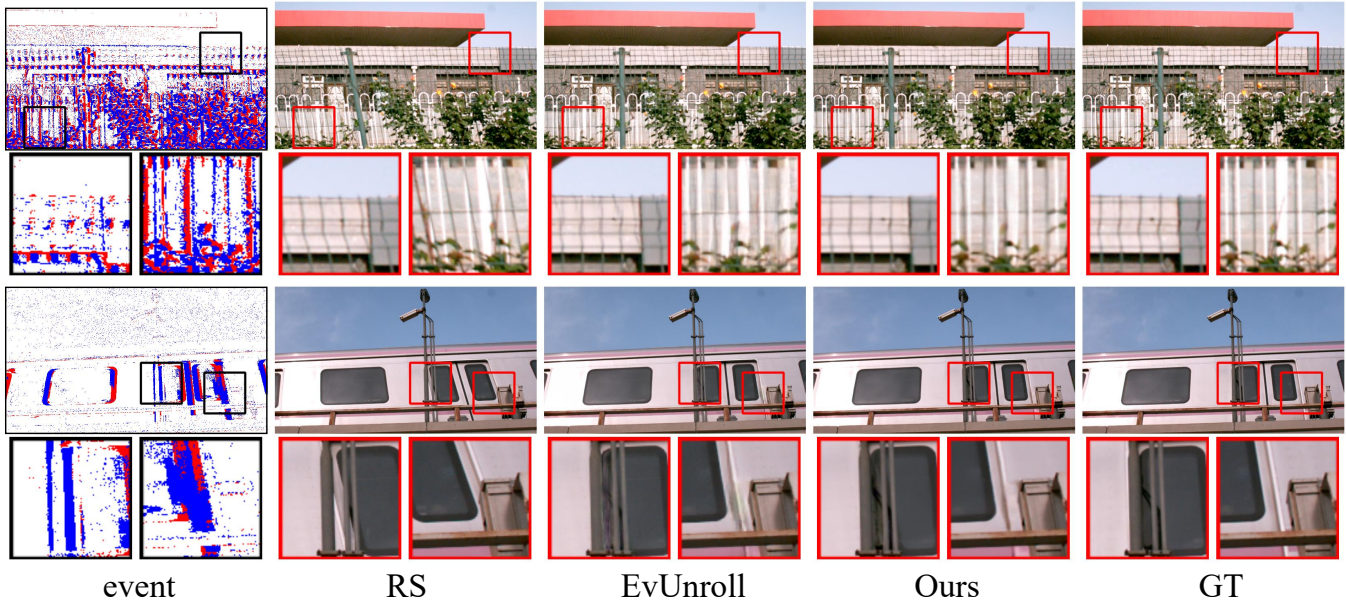


Figure 5: Visual comparison on Gev-RS dataset. The event frame is generated by the events within the neighborhood of the GS timestamp. The displayed ground truth (GT) in the images corresponds to the mid-exposure time in RS.

fusion, directly fusing these two can not extract precise temporal information. In scenarios with high requirement on time accuracy, such as high-speed motion, it may lead to local blur in the restored output.

Table 2: Results on Gev-RS.

Methods	events	PSNR	SSIM	LPIPS
DSUN [15]	✗	23.10	0.70	0.166
JCD [31]	✗	24.90	0.82	0.105
IFED [30]	✗	27.16	0.85	0.097
SelfDRSC [19]	✗	26.58	0.84	0.113
JAMNet [5]	✗	27.02	0.85	0.105
EvUnroll [32]	✓	32.16	0.91	0.061
ours	✓	<b>33.53</b>	<b>0.92</b>	<b>0.021</b>

## 4.2 Experiments on Gev-RS dataset

Gev-RS collects GS videos by using a high-speed camera at 5700 fps. Then GS videos are fed into the event simulator V2E [8] to obtain event data, and generate RS images based on Eq. 3 with  $640 \times 360$  resolution.

In Fig. 5, we compare our method with EvUnroll [32] on Gev-RS dataset. The resulting images in the figure are all GS images at the intermediate exposure time of RS images. In the first case, it can be clearly seen that Evunroll produces artifacts when the foreground and background are close, such as the region between the metal box and the train. Additionally, it also failed to accurately reproduce the reflection of the lamp post in the window.

This is caused by event overlap between the foreground and background. Our approach effectively integrates the two modalities, enabling model to distinguish whether the event is generated by the foreground or background. As a result, our method can avoid the occurrence of similar artifacts. The second example is highly challenging, involving complex scenes with moving objects. Both the small green and white fence in the foreground are difficult targets for restoration. While EvUnroll’s recovery of the white fence appears slightly blurred and the green fence exhibits disjointed segments, our method can accurately capture the displacement of small objects to restore the green fence and also recover the white fence without being affected by high-speed motion. Finally, as shown in Tab. 2, we outperform EvUnroll by 1.37 dB in PSNR, 0.040 in terms of LPIPS [28] and far superior to other image based methods.

Table 3: Results on Fastec-RS.

Methods	events	PSNR	SSIM	LPIPS
DSUN [15]	✗	26.73	0.82	0.166
JCD [31]	✗	26.48	0.82	0.105
SUNet [3]	✗	27.06	0.83	-
JAMNet [5]	✗	28.70	0.87	0.093
EvUnroll [32]	✓	31.32	0.88	<b>0.061</b>
EvShutter [1]	✓	32.41	<b>0.91</b>	<b>0.061</b>
ours	✓	<b>32.51</b>	<b>0.91</b>	0.070

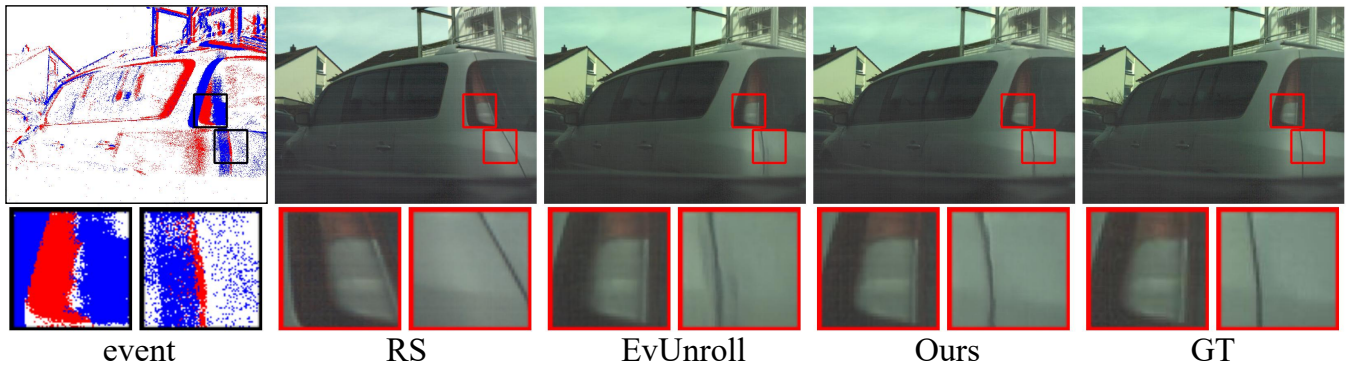


Figure 6: Visual comparison on Fastec-RS dataset. The event frame is generated by the events within the neighborhood of the GS timestamp. The displayed ground truth (GT) in the images corresponds to the mid-exposure time in RS.

### 4.3 Experiments on Fastec-RS dataset

Fastec-RS collects GS images at 2400 fps with  $640 \times 480$  resolution, and then simulate event data and RS image in the same way as Gev-RS.

In Fig. 6, We compare our method with EvUnroll [32]. When an object moves too close to the camera, causing significant relative movement, EvUnroll produces noticeable artifacts. Even though evunroll utilizes a dual-branch structure, its warping branch fails under significant displacements, while the synthesis branch lacks detailed handling of temporal information in events. Consequently, when a large number of events occur within a short period due to high-speed motion, the accumulation of unnecessary events leads to blurring. In our method, each head of the TMA focuses on event information at different time frames, enabling us to better address the challenges presented by highly dynamic movements.

As shown in Tab. 3, Our method outperform EvUnroll by 1.16 dB in PSNR but only exhibits only a slight superiority over EvShutter [1]. More results compared with image-based methods on Gev-RS and Fastec-RS will be shown in Supp. Mat..

Table 4: Results on different methods with our self-supervised learning.

Dataset	Methods	PSNR	SSIM
Gev-RS	EvUnroll	32.16	0.91
	EvUnroll(u)	33.49	<b>0.92</b>
Gev-RS	ours	33.53	<b>0.92</b>
	ours(u)	<b>33.92</b>	<b>0.92</b>

### 4.4 Experiments on self-supervision

To validate the effectiveness of self-supervised learning, we conducted experiments on both the test set of a synthetic dataset and a real-world dataset.

As shown in Fig. 7, the left image is the result of training with self-supervised function, while the right image is reversed. With self-supervised learning, the model learned partial data distribution of the test set and removed the artifacts caused by incomplete

restoration, leading to better performance and a 0.49 dB improvement in PSNR. Additionally, we applied the self-supervised loss to EvUnroll, resulting in a 1.33 dB boost, as shown in Tab. 4. This demonstrates the broad applicability of our self-supervised function, which can be applied to different multi-modality methods.

Furthermore, in the Fig. 1 and Fig. 8, we present the results on a real dataset collected by EvUnroll. The yellow dashed line is the GS reference line drawn based on the intermediate event. The initial results with ghosting effects were not good, possibly due to dataset gaps, but after the self-supervised learning, the image quality gradually improved. In the case of building, the boundary the building restored by EvUnroll is quite blurry, as analyzed earlier, primarily due to the limited use of detailed temporal information. Moreover, the restored windows exhibit ghosting and distortion in the glass. Our method outperforms EvUnroll in edge restoration, but it still exhibits ghosting in the windows. Nevertheless, the addition of self-supervised learning results in remarkably clear window restoration. In the next case, self-supervised learning eliminates the direct artifacts between the stick and the base, and prevents the occurrence of puppet distortion in the results of evunroll. It is noteworthy that fine-tuning from the weights pretrained on the synthetic data on real data typically requires just a few hundred iterations.

Both the results on real-world and synthetic datasets demonstrate the effectiveness of the proposed self-supervised loss.



Figure 7: Visual comparison of self-supervised learning.

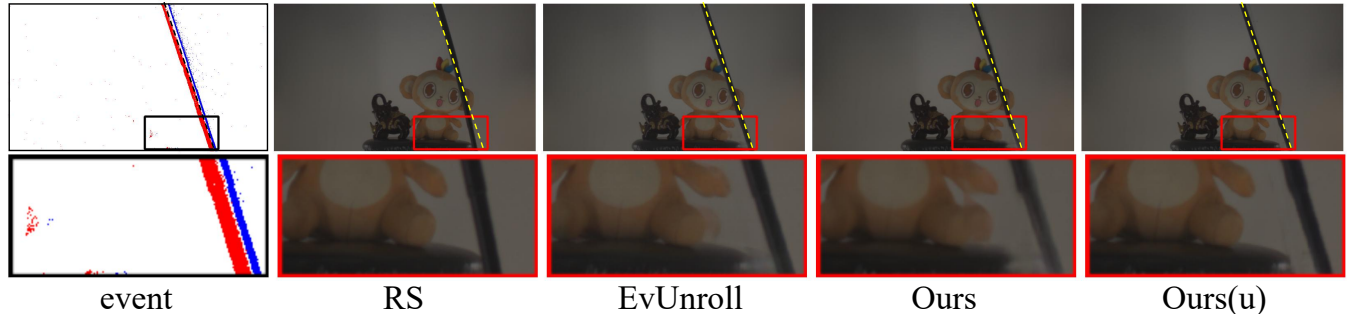


Figure 8: Visual comparison on real-world dataset. The yellow dashed line is the GS reference line drawn based on the intermediate event. The label (u) means fine-tuning using self-supervised learning.

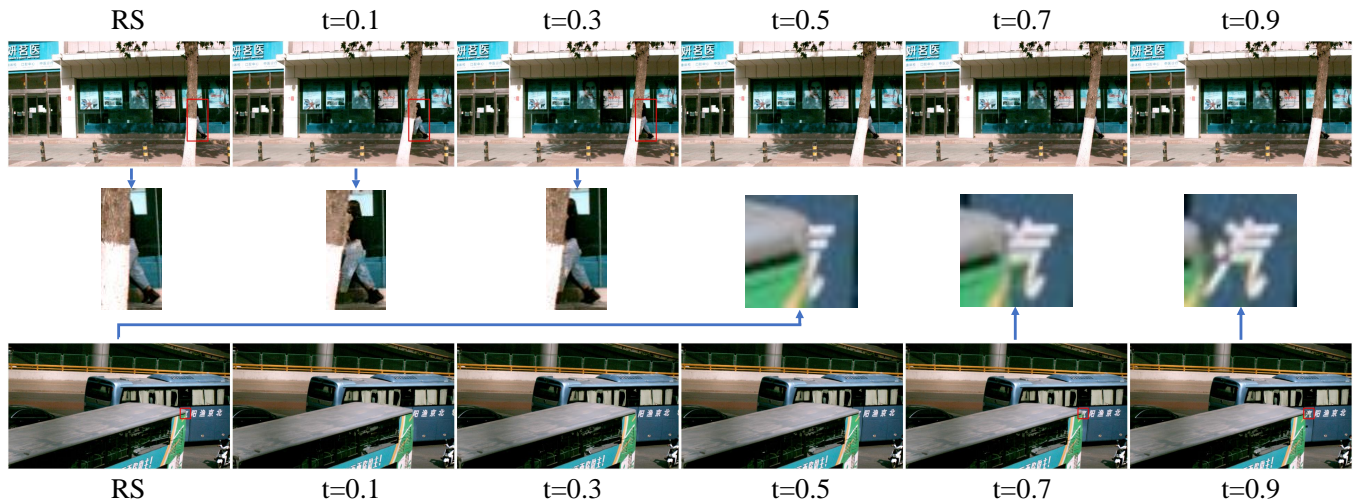


Figure 9: Visual comparison on arbitrary timestamp.

#### 4.5 Experiments on arbitrary timestamp

To validate the effectiveness of Time-Aware Attention, GS images at different timestamps are generated. As shown in Fig. 9, we present two scenarios, with one featuring a person occluded by trees and the other with text occluded by a bus. Despite occlusions of text and persons by the foreground in the RS images, these areas are effectively recovered.

Table 5: Performance(PSNR) on different timestamps.

timestamp	0.1	0.3	0.5	0.7	0.9
ours	32.06	32.38	33.53	33.74	32.41
EvUnroll	31.40	32.04	32.16	32.40	31.78

Additionally, we conduct a quantitative comparison with EvUnroll across different timestamps in Tab. 5. It can be observed that performance decreases as the timestamp  $t$  approaches the start or end of the RS exposure time ( $t = 0.1, 0.9$ ). This is because at these moments, the temporal span between RS and GS at the bottom/top of

the image is too large (nearly the whole RS exposure time), leading to poor local reconstruction. In contrast, at the mid-exposure time ( $t = 0.5$ ), the temporal span is relatively smaller (half of the whole RS exposure time). The larger the difference is, the more challenging the RSC task is. As shown in Tab. 5, our method outperforms EvUnroll at all timestamps.

## 5 CONCLUSION

In this work, we propose an encoder-decoder framework for the RSC task. In encoder, we design time encoding as a bridge for the interaction of two modalities, and skillfully integrate it with multi-head attention to make more intricate use of temporal information. In decoder, we use the existing DCA module to integrate motion information of event and appearance information of RS, and employed the GS time encoding as a query for decoding. Additionally, we develop self-supervised loss specific to the RSC task and confirm its effectiveness on both synthetic and real datasets. Our method outperforms existing methods in both qualitative and quantitative performance.

## REFERENCES

- [1] Julius Erbach, Stepan Tulyakov, Patricia Vitoria, Alfredo Boicichio, and Yuanyou Li. 2023. EvShutter: Transforming Events for Unconstrained Rolling Shutter Correction. In *IEEE/CVF Conference on Computer Vision and Pattern Recognition, CVPR 2023, Vancouver, BC, Canada, June 17-24, 2023*. IEEE, 13904–13913. <https://doi.org/10.1109/CVPR52729.2023.01336>
- [2] Bin Fan and Yuchao Dai. 2021. Inverting a Rolling Shutter Camera: Bring Rolling Shutter Images to High Framerate Global Shutter Video. In *2021 IEEE/CVF International Conference on Computer Vision, ICCV 2021, Montreal, QC, Canada, October 10-17, 2021*. IEEE, 4208–4217. <https://doi.org/10.1109/ICCV48922.2021.00419>
- [3] Bin Fan, Yuchao Dai, and Mingyi He. 2021. SUNet: Symmetric Undistortion Network for Rolling Shutter Correction. In *2021 IEEE/CVF International Conference on Computer Vision, ICCV 2021, Montreal, QC, Canada, October 10-17, 2021*. IEEE, 4521–4530. <https://doi.org/10.1109/ICCV48922.2021.00450>
- [4] Bin Fan, Yuchao Dai, Zhiyuan Zhang, Qi Liu, and Mingyi He. 2022. Context-Aware Video Reconstruction for Rolling Shutter Cameras. In *IEEE/CVF Conference on Computer Vision and Pattern Recognition, CVPR 2022, New Orleans, LA, USA, June 18-24, 2022*. IEEE, 17551–17561. <https://doi.org/10.1109/CVPR52688.2022.01705>
- [5] Bin Fan, Yuxin Mao, Yuchao Dai, Zhexiong Wan, and Qi Liu. 2023. Joint Appearance and Motion Learning for Efficient Rolling Shutter Correction. In *IEEE/CVF Conference on Computer Vision and Pattern Recognition, CVPR 2023, Vancouver, BC, Canada, June 17-24, 2023*. IEEE, 5671–5681. <https://doi.org/10.1109/CVPR52729.2023.00549>
- [6] Guillermo Gallego, Tobi Delbrück, Garrick Orchard, Chiara Bartolozzi, Brian Taba, Andrea Censi, Stefan Leutenegger, Andrew J. Davison, Jörg Conradt, Kostas Daniilidis, and Davide Scaramuzza. 2022. Event-Based Vision: A Survey. *IEEE Trans. Pattern Anal. Mach. Intell.* 44, 1 (2022), 154–180. <https://doi.org/10.1109/TPAMI.2020.3008413>
- [7] Weihua He, Kaichao You, Zhendong Qiao, Xu Jia, Ziyang Zhang, Wenhui Wang, Huchuan Lu, Yaoyuan Wang, and Jianxing Liao. 2022. TimeReplayer: Unlocking the Potential of Event Cameras for Video Interpolation. In *IEEE/CVF Conference on Computer Vision and Pattern Recognition, CVPR 2022, New Orleans, LA, USA, June 18-24, 2022*. IEEE, 17783–17792. <https://doi.org/10.1109/CVPR52688.2022.01728>
- [8] Yuhuang Hu, Shih-Chii Liu, and Tobi Delbrück. 2021. v2e: From Video Frames to Realistic DVS Events. In *IEEE Conference on Computer Vision and Pattern Recognition Workshops, CVPR Workshops 2021, virtual, June 19-25, 2021*. Computer Vision Foundation / IEEE, 1312–1321. <https://doi.org/10.1109/CVPRW53098.2021.00144>
- [9] Huaizu Jiang, Deqing Sun, Varun Jampani, Ming-Hsuan Yang, Erik G. Learned-Miller, and Jan Kautz. 2018. Super SloMo: High Quality Estimation of Multiple Intermediate Frames for Video Interpolation. In *2018 IEEE Conference on Computer Vision and Pattern Recognition, CVPR 2018, Salt Lake City, UT, USA, June 18-22, 2018*. Computer Vision Foundation / IEEE Computer Society, 9000–9008. <https://doi.org/10.1109/CVPR.2018.00938>
- [10] Zhe Jiang, Yu Zhang, Dongqing Zou, Jimmy S. J. Ren, Jiancheng Lv, and Yebin Liu. 2020. Learning Event-Based Motion Deblurring. In *2020 IEEE/CVF Conference on Computer Vision and Pattern Recognition, CVPR 2020, Seattle, WA, USA, June 13-19, 2020*. Computer Vision Foundation / IEEE, 3317–3326. <https://doi.org/10.1109/CVPR42600.2020.00338>
- [11] Justin Johnson, Alexandre Alahi, and Li Fei-Fei. 2016. Perceptual Losses for Real-Time Style Transfer and Super-Resolution. In *Computer Vision - ECCV 2016 - 14th European Conference, Amsterdam, The Netherlands, October 11-14, 2016, Proceedings, Part II (Lecture Notes in Computer Science, Vol. 9906)*, Bastian Leibe, Jiri Matas, Nicu Sebe, and Max Welling (Eds.). Springer, 694–711. [https://doi.org/10.1007/978-3-319-46475-6\\_43](https://doi.org/10.1007/978-3-319-46475-6_43)
- [12] Taewoo Kim, Yujeong Chae, Hyun-Kurl Jang, and Kuk-Jin Yoon. 2023. Event-based Video Frame Interpolation with Cross-Modal Asymmetric Bidirectional Motion Fields. In *IEEE/CVF Conference on Computer Vision and Pattern Recognition, CVPR 2023, Vancouver, BC, Canada, June 17-24, 2023*. IEEE, 18032–18042. <https://doi.org/10.1109/CVPR52729.2023.01729>
- [13] Jingyun Liang, Jiezhang Cao, Guolei Sun, Kai Zhang, Luc Van Gool, and Radu Timofte. 2021. SwinIR: Image Restoration Using Swin Transformer. In *IEEE/CVF International Conference on Computer Vision Workshops, ICCVW 2021, Montreal, BC, Canada, October 11-17, 2021*. IEEE, 1833–1844. <https://doi.org/10.1109/ICCVW54120.2021.00210>
- [14] Songnan Lin, Jiawei Zhang, Jinshan Pan, Zhe Jiang, Dongqing Zou, Yongtian Wang, Jing Chen, and Jimmy S. J. Ren. 2020. Learning Event-Driven Video Deblurring and Interpolation. In *Computer Vision - ECCV 2020 - 16th European Conference, Glasgow, UK, August 23-28, 2020, Proceedings, Part VIII (Lecture Notes in Computer Science, Vol. 12353)*, Andrea Vedaldi, Horst Bischof, Thomas Brox, and Jan-Michael Frahm (Eds.). Springer, 695–710. [https://doi.org/10.1007/978-3-030-58598-3\\_41](https://doi.org/10.1007/978-3-030-58598-3_41)
- [15] Peidong Liu, Zhaopeng Cui, Viktor Larsson, and Marc Pollefeys. 2020. Deep Shutter Unrolling Network. In *2020 IEEE/CVF Conference on Computer Vision and Pattern Recognition, CVPR 2020, Seattle, WA, USA, June 13-19, 2020*. Computer Vision Foundation / IEEE, 5940–5948. <https://doi.org/10.1109/CVPR42600.2020.00598>
- [16] Depu Meng, Xiaokang Chen, Zejia Fan, Gang Zeng, Houqiang Li, Yuhui Yuan, Lei Sun, and Jingdong Wang. 2021. Conditional DETR for Fast Training Convergence. In *2021 IEEE/CVF International Conference on Computer Vision, ICCV 2021, Montreal, QC, Canada, October 10-17, 2021*. IEEE, 3631–3640. <https://doi.org/10.1109/ICCV48922.2021.00363>
- [17] Eyal Naor, Itai Antebi, Shai Bagon, and Michal Irani. 2022. Combining Internal and External Constraints for Unrolling Shutter in Videos. In *Computer Vision - ECCV 2022 - 17th European Conference, Tel Aviv, Israel, October 23-27, 2022, Proceedings, Part XVII (Lecture Notes in Computer Science, Vol. 13677)*, Shai Avidan, Gabriel J. Brostow, Moustapha Cissé, Giovanni Maria Farinella, and Tal Hassner (Eds.). Springer, 119–134. [https://doi.org/10.1007/978-3-031-19790-1\\_8](https://doi.org/10.1007/978-3-031-19790-1_8)
- [18] Liyuan Pan, Cedric Scheerlinck, Xin Yu, Richard Hartley, Miaomiao Liu, and Yuchao Dai. 2019. Bringing a Blurry Frame Alive at High Frame-Rate With an Event Camera. In *IEEE Conference on Computer Vision and Pattern Recognition, CVPR 2019, Long Beach, CA, USA, June 16-20, 2019*. Computer Vision Foundation / IEEE, 6820–6829. <https://doi.org/10.1109/CVPR.2019.00698>
- [19] Wei Shang, Dongwei Ren, Chaoyu Feng, Xiaotao Wang, Lei Lei, and Wangmeng Zuo. 2023. Self-supervised Learning to Bring Dual Reversed Rolling Shutter Images Alive. In *IEEE/CVF International Conference on Computer Vision, ICCV 2023, Paris, France, October 1-6, 2023*. IEEE, 13040–13048. <https://doi.org/10.1109/ICCV51070.2023.01203>
- [20] Chen Song, Qixing Huang, and Chandrajit Bajaj. 2022. E-CIR: Event-Enhanced Continuous Intensity Recovery. In *IEEE/CVF Conference on Computer Vision and Pattern Recognition, CVPR 2022, New Orleans, LA, USA, June 18-24, 2022*. IEEE, 7793–7802. <https://doi.org/10.1109/CVPR52688.2022.00765>
- [21] Lei Sun, Christos Sakaridis, Jingyun Liang, Qi Jiang, Kailun Yang, Peng Sun, Yaozu Ye, Kaiwei Wang, and Luc Van Gool. 2022. Event-Based Fusion for Motion Deblurring with Cross-modal Attention. In *Computer Vision - ECCV 2022 - 17th European Conference, Tel Aviv, Israel, October 23-27, 2022, Proceedings, Part XVIII (Lecture Notes in Computer Science, Vol. 13678)*, Shai Avidan, Gabriel J. Brostow, Moustapha Cissé, Giovanni Maria Farinella, and Tal Hassner (Eds.). Springer, 412–428. [https://doi.org/10.1007/978-3-031-19797-0\\_24](https://doi.org/10.1007/978-3-031-19797-0_24)
- [22] Lei Sun, Christos Sakaridis, Jingyun Liang, Peng Sun, Kai Zhang, Jiezhang Cao, Qi Jiang, Kaiwei Wang, and Luc Van Gool. 2023. Event-Based Frame Interpolation with Ad-hoc Deblurring. In *IEEE/CVF Conference on Computer Vision and Pattern Recognition, CVPR 2023, Vancouver, BC, Canada, June 17-24, 2023*. IEEE, 18043–18052. <https://doi.org/10.1109/CVPR52729.2023.01730>
- [23] Stepan Tulyakov, Alfredo Boicichio, Daniel Gehrig, Stamatios Georgoulis, Yuanyou Li, and Davide Scaramuzza. 2022. Time Lens++: Event-based Frame Interpolation with Parametric Nonlinear Flow and Multi-scale Fusion. In *IEEE/CVF Conference on Computer Vision and Pattern Recognition, CVPR 2022, New Orleans, LA, USA, June 18-24, 2022*. IEEE, 17734–17743. <https://doi.org/10.1109/CVPR52688.2022.01723>
- [24] Stepan Tulyakov, Daniel Gehrig, Stamatios Georgoulis, Julius Erbach, Mathias Gehrig, Yuanyou Li, and Davide Scaramuzza. 2021. Time Lens: Event-Based Video Frame Interpolation. In *IEEE Conference on Computer Vision and Pattern Recognition, CVPR 2021, virtual, June 19-25, 2021*. Computer Vision Foundation / IEEE, 16155–16164. <https://doi.org/10.1109/CVPR46437.2021.01589>
- [25] Ashish Vaswani, Noam Shazeer, Niki Parmar, Jakob Uszkoreit, Llion Jones, Aidan N. Gomez, Lukasz Kaiser, and Illia Polosukhin. 2017. Attention is All you Need. In *Advances in Neural Information Processing Systems 30: Annual Conference on Neural Information Processing Systems 2017, December 4-9, 2017, Long Beach, CA, USA, Isabelle Guyon, Ulrike von Luxburg, Samy Bengio, Hanna M. Wallach, Rob Fergus, S. V. N. Vishwanathan, and Roman Garnett (Eds.)*. 5998–6008. <https://proceedings.neurips.cc/paper/2017/hash/3f5ee243547dee91fbd053c1c4a845aa-Abstract.html>
- [26] Song Wu, Kaichao You, Weihua He, Chen Yang, Yang Tian, Yaoyuan Wang, Ziyang Zhang, and Jianxing Liao. 2022. Video Interpolation by Event-Driven Anisotropic Adjustment of Optical Flow. In *Computer Vision - ECCV 2022 - 17th European Conference, Tel Aviv, Israel, October 23-27, 2022, Proceedings, Part VII (Lecture Notes in Computer Science, Vol. 13667)*, Shai Avidan, Gabriel J. Brostow, Moustapha Cissé, Giovanni Maria Farinella, and Tal Hassner (Eds.). Springer, 267–283. [https://doi.org/10.1007/978-3-031-20071-7\\_16](https://doi.org/10.1007/978-3-031-20071-7_16)
- [27] Fang Xu, Lei Yu, Bishan Wang, Wen Yang, Gui-Song Xia, Xu Jia, Zhendong Qiao, and Jianzhuang Liu. 2021. Motion Deblurring with Real Events. In *2021 IEEE/CVF International Conference on Computer Vision, ICCV 2021, Montreal, QC, Canada, October 10-17, 2021*. IEEE, 2563–2572. <https://doi.org/10.1109/ICCV48922.2021.00258>
- [28] Richard Zhang, Phillip Isola, Alexei A. Efros, Eli Shechtman, and Oliver Wang. 2018. The Unreasonable Effectiveness of Deep Features as a Perceptual Metric. In *2018 IEEE Conference on Computer Vision and Pattern Recognition, CVPR 2018, Salt Lake City, UT, USA, June 18-22, 2018*. Computer Vision Foundation / IEEE Computer Society, 586–595. <https://doi.org/10.1109/CVPR.2018.00068>
- [29] Xiang Zhang and Lei Yu. 2022. Unifying Motion Deblurring and Frame Interpolation with Events. In *IEEE/CVF Conference on Computer Vision and Pattern Recognition, CVPR 2022, New Orleans, LA, USA, June 18-24, 2022*. IEEE, 17744–17753. <https://doi.org/10.1109/CVPR52688.2022.01724>

929  
930  
931  
932  
933  
934  
935  
936  
937  
938  
939  
940  
941  
942  
943  
944  
945  
946  
947  
948  
949  
950  
951  
952  
953  
954  
955  
956  
957  
958  
959  
960  
961  
962  
963  
964  
965  
966  
967  
968  
969  
970  
971  
972  
973  
974  
975  
976  
977  
978  
979  
980  
981  
982  
983  
984  
985  
986987  
988  
989  
990  
991  
992  
993  
994  
995  
996  
997  
998  
999  
1000  
1001  
1002  
1003  
1004  
1005  
1006  
1007  
1008  
1009  
1010  
1011  
1012  
1013  
1014  
1015  
1016  
1017  
1018  
1019  
1020  
1021  
1022  
1023  
1024  
1025  
1026  
1027  
1028  
1029  
1030  
1031  
1032  
1033  
1034  
1035  
1036  
1037  
1038  
1039  
1040  
1041  
1042  
1043  
1044

1045	[30]	Zhihang Zhong, Mingdeng Cao, Xiao Sun, Zhirong Wu, Zhongyi Zhou, Yinqiang Zheng, Stephen Lin, and Imari Sato. 2022. Bringing Rolling Shutter Images Alive with Dual Reversed Distortion. In <i>Computer Vision - ECCV 2022 - 17th European Conference, Tel Aviv, Israel, October 23-27, 2022, Proceedings, Part VII (Lecture Notes in Computer Science, Vol. 13667)</i> , Shai Avidan, Gabriel J. Brostow, Moustapha Cissé, Giovanni Maria Farinella, and Tal Hassner (Eds.). Springer, 233–249. <a href="https://doi.org/10.1007/978-3-031-20071-7_14">https://doi.org/10.1007/978-3-031-20071-7_14</a>	1103
1046			1104
1047			1105
1048			1106
1049			1107
1050	[31]	Zhihang Zhong, Yinqiang Zheng, and Imari Sato. 2021. Towards Rolling Shutter Correction and Deblurring in Dynamic Scenes. In <i>IEEE Conference on Computer Vision and Pattern Recognition, CVPR 2021, virtual, June 19-25, 2021</i> . Computer Vision Foundation / IEEE, 9219–9228. <a href="https://doi.org/10.1109/CVPR46437.2021.00910">https://doi.org/10.1109/CVPR46437.2021.00910</a>	1108
1051			1109
1052			1110
1053			1111
1054	[32]	Xinyu Zhou, Peiqi Duan, Yi Ma, and Boxin Shi. 2022. EvUnroll: Neuromorphic Events based Rolling Shutter Image Correction. In <i>IEEE/CVF Conference on Computer Vision and Pattern Recognition, CVPR 2022, New Orleans, LA, USA, June 18-24, 2022</i> . IEEE, 17754–17763. <a href="https://doi.org/10.1109/CVPR52688.2022.01725">https://doi.org/10.1109/CVPR52688.2022.01725</a>	1112
1055			1113
1056			1114
1057			1115
1058			1116
1059			1117
1060			1118
1061			1119
1062			1120
1063			1121
1064			1122
1065			1123
1066			1124
1067			1125
1068			1126
1069			1127
1070			1128
1071			1129
1072			1130
1073			1131
1074			1132
1075			1133
1076			1134
1077			1135
1078			1136
1079			1137
1080			1138
1081			1139
1082			1140
1083			1141
1084			1142
1085			1143
1086			1144
1087			1145
1088			1146
1089			1147
1090			1148
1091			1149
1092			1150
1093			1151
1094			1152
1095			1153
1096			1154
1097			1155
1098			1156
1099			1157
1100			1158
1101			1159
1102			1160
	[33]	Alex Zihao Zhu, Liangzhe Yuan, Kenneth Chaney, and Kostas Daniilidis. 2018. Unsupervised Event-Based Optical Flow Using Motion Compensation. In <i>Computer Vision - ECCV 2018 Workshops - Munich, Germany, September 8-14, 2018, Proceedings, Part VI (Lecture Notes in Computer Science, Vol. 11134)</i> , Laura Leal-Taixé and Stefan Roth (Eds.). Springer, 711–714. <a href="https://doi.org/10.1007/978-3-030-11024-6_54">https://doi.org/10.1007/978-3-030-11024-6_54</a>	1160
			1161
	[34]	Xizhou Zhu, Weijie Su, Lewei Lu, Bin Li, Xiaogang Wang, and Jifeng Dai. 2021. Deformable DETR: Deformable Transformers for End-to-End Object Detection. In <i>9th International Conference on Learning Representations, ICLR 2021, Virtual Event, Austria, May 3-7, 2021</i> . OpenReview.net. <a href="https://openreview.net/forum?id=gZ9hCDWe6ke">https://openreview.net/forum?id=gZ9hCDWe6ke</a>	1162